Superkurtosis

Degiannakis, Stavros and Filis, George and Siourounis, Grigorios and Trapani, Lorenzo

Panteion University of Social and Political Sciences, Greece, University of Patras, Greece, Panteion University of Social and Political Sciences, Greece, University of Nottingham, UK

16 October 2021

Superkurtosis

Stavros Degiannakis[*] **George Filis**[†] **Grigorios Siourounis**[‡] **Lorenzo Trapani**[§]

Abstract:

Very little is known on how traditional risk metrics behave under intraday trading. We fill this void by examining the finiteness of the returns' moments and assessing the impact of their infinity in a risk management framework. We show that when intraday trading is considered, assuming finite higher order moments, potential losses are materially larger than what the theory predicts, and they increase exponentially as the trading frequency increases - a phenomenon we call *superkurtosis*. Hence, the use of the current risk management techniques under intraday trading impose threats to the stability of financial markets, given that capital ratios may be severely underestimated.

———————————————

[*]Panteion University of Social and Political Science, and Bank of Greece. Email: stavros.degiannakis@gmail.com.

[†]University of Patras. Email: gfilis@upatras.gr.

[‡]Panteion University of Social and Political Science, and Brown University. Email: grigorios_siourounis@brown.edu.

[§]University of Nottingham. Email: lorenzo.trapani@nottingham.ac.uk.

1. Introduction

Highly sophisticated algorithms and fast computer technology have originated a new class of trading known as "intraday trading". Intraday trading has numerous advantages: it offers a great deal of liquidity in the market; it facilitates the instantaneous transmission of information into prices, pushing markets to be more efficient; and it creates a market place for small (retail) as well as large investors (institutions).

However, intraday trading also presents unique challenges (see for example the Final Project Report from The Government Office for Science, London - 2012). Chiefly, it has been criticised as liable to cause large market crashes which may be amplified by the influx of algorithmic trading and the order clustering caused by unintended trading strategy coordination (see e.g. Beddington et al., 2012; Kirilenko et al., 2017; Manhire, 2018; and media coverage such as Brush et al., 2015). Hence, regulators (see the Press Release, European Parliament, MEPs Vote Laws to Regulate Financial Markets and Curb High Frequency Trading (Apr. 15, 2014)), economists (e.g. Kirilenko and Lo, 2013) and law scholars (e.g. Yadav, 2015) have proposed measures to mitigate such trading behaviour.

As a consequence of the issues discussed above, market participants are required to measure and report several market risk metrics, and to take them into account when calculating their regulated capital requirements. For example, on January 16th, 2016 the Basel Committee on Banking Supervision (henceforth, "the Commitee") published a document that revised standards for minimum capital requirements for Market Risk. In addition, the Committee had also produced three consultative papers on the Fundamental review of the trading book, namely (i) Fundamental review of the trading book, May 2012, (ii) A revised market risk framework, October 2013 and (iii) Fundamental review of the trading book: Outstanding issues, December 2014. Furthermore, ECB imposes capital requirements (via the Capital Requirements Regulation) on institutions who engage in intraday trading. Such requirements are based on risk metrics or asset volatility.[1] However, standards set by regulators are based

---

[1] For details see https://www.bankingsupervision.europa.eu/press/publications/newsletter/2019/html/ssm.nl190213-

on risk metrics that are calculated - at most - at daily frequency. Given that intraday trading takes place at higher frequencies, this leaves the market risk, generated by such trading activity, largely as a dark pool. Indeed, very little is known about market risk associated with intraday trading; similarly, only little analysis has been conducted on how traditional risk metrics such as Value-at-Risk (VaR, hereafter) or Expected Shortfall (ES, hereafter) behave at such high frequency trading. The investigation of this issue is arguably of immense importance, due to the fact that typical risk metrics users assume that high order moments of asset returns at intraday frequency are finite. This assumptions is based on the fact that such moments are finite at lower, e.g. daily, frequency, which may be not hold true for higher frequencies. Consequently, the VaR and ES are calculated under the assumptions that high order moments are finite, typically using the quantiles of the normal distribution. In turn, such risk metrics computations are assumed to adequately capture capital requirements, which may be grossly incorrect in the presence of heavy tails. Of course, it is perfectly possible to compute the VaR and ES without assuming normality. However, existing methodologies require several assumptions which may not be satisfied: for example, Extreme Value Theory based methodologies usually require the *i.i.d.* assumption (see Manganelli and Engle, 2001), which is highly unlikely to be satisfied by intraday returns. Thus, prior to calculating any risk metric, it is of vital importance to have a deep understanding of the properties of the data. Despite its importance, the assumption of finite moments has not been formally tested thus far to the best of our knowledge.

In this study, we fill the gaps discussed above by offering two contributions. Firstly, we develop a methodology to check whether high order moments are finite. We point out that, in this context, very few tests are available. One exception is Trapani (2016), but his test (as we discuss in more detail below) produces non replicable results, so that different researchers using the same datasets may obtain different results as to the finiteness, or not, of high order moments. Conversely, our methodology overcomes this issue, ensuring that all researchers using the same dataset will obtain the same results and draw the same conclusions. As a

5.en.html

second contribution, we assess the impact of having infinite moments in a risk management framework. In our empirical analysis, we focus on the foreign exchange market, which is justified by the fact that - in that context - trading has become increasingly electronic and automated. The use of intraday frequency algorithms and machine learning protocols are continuously increasing in the foreign exchange market with more than 65% of the more than 5 trillion dollars daily volume to be traded from such algorithms. In addition, more than 80% of Central Banks monitor Fasted Paced Electronic Markets operations and 60% is for market stability reasons alone.

In our empirical analysis (Section 3), we apply our test to check whether the first four moments are finite, using intraday data from the currency markets. We find that the distribution of the returns of the assets traded intraday does not have finite absolute moments of order higher than 3,[2] implying that mainly the kurtosis is infinite at intraday frequencies. In contrast, daily data do have finite moments. The finiteness of high order moments at lower frequencies may explain why the traditional, Gaussian-based way of computing VaR and ES is used also at high frequency. However, using a distribution which admits all moments in the presence of heavy tails may lead to wrong conclusions: in Section 3.3, we illustrate the consequences of neglecting this feature, calculating the high losses incurred by (and the short survival of) an investor who ignores this issue. In order to shed further light, in Section 4 we report extensive Monte Carlo evidence showing that VaR and ES are much larger than implied e.g. by the classical risk management approaches. We find that this is due to two reasons. First, the natural increase in the sample size as the frequency increases directly affects potential losses. Secondly, we find clear numerical evidence that, at higher frequencies, data sampled from a distribution which has heavy tails tend to have higher sample moments (chiefly, higher kurtosis) than the theory would predict.[3] In turn, this affects the potential

---

[2]We note that there are intraday frequencies which exhibit infinite third moment. However, our analysis is focused on the severe implications brought about by the fourth moment being infinite in intraday frequencies, since our testing and simulations show that even when the 3rd moment is infinite, this does not alter the VaR or ES metrics in any statistically significant manner.

[3]This consideration is based on the Marcinkiewicz-Zygmund SLLN, which provides an upper bound on

losses associated with VaR or ES. In order to confirm this striking empirical finding, and to disentangle possible sources of the extreme (infinite) potential losses, we carry out an extensive series of simulations. Evidence from simulated data suggests that, on one hand, the estimated kurtosis grows as the sampling frequency increases (as the Strong Law of Large Numbers - SLLN henceforth - implies), yet, on the other hand, the growth pattern exhibits a much faster rate than the one implied by the SLLN bound. Thus, kurtosis diverges much faster from its theoretical path as the sampling frequency increases, contributing significantly to the increase of the potential losses at intraday trading. Hence, the simulated data lend strong support to our empirical conclusions generated from the use of actual currency pairs data. We call this phenomenon *superkurtosis*; it implies that traditional risk metrics are not a good measure for the true market risk (see also Bradley and Taqqu, 2003), and should therefore not be employed to gauge capital adequacy under intraday trading.

The remainder of the paper is organised as follows. Section 2 describes the methods used for the test of moments, as well as, for the assessment of the impact of these moments on risk management. Section 3 presents our empirical results from the real data and Section 4 for the simulated data. Finally, Section 5 concludes the study and provides ideas for future research. Technical results and further tables are in the appendix.

2. Methodology

Our methodology consists of two steps. We start by verifying whether higher order moments are finite (Section 2.1); we then turn to assessing the impact of having infinite high order moments on risk metrics (Section 2.2).

2.1. Testing for the finiteness of the asset returns' moments.

In this section, we discuss testing for the finiteness of the moments of a random variable X, given a sample $\{x_t\}_{t=1}^T$, also proposing an improved, replicable version of the original test by

---

the growth rate of sample moments when the corresponding population moments are infinite.

Trapani (2016) - see below for details. Our hypothesis testing framework is as follows:

$$
\begin{cases}
H_0 : E\,|X|^k = \infty \\
H_A : E\,|X|^k < \infty
\end{cases}
,
\tag{2.1}
$$

with $k = 2$, 3 and 4. In (2.1), the null hypothesis is the *infinity* of the k-th absolute moment. As in Trapani (2016), for each k, test statistics are based on

$$
\mu_k = c_k \times \frac{T^{-1}\sum_{t=1}^{T} |x_t|^k}{\left(T^{-1}\sum_{t=1}^{T} |x_t|^p\right)^{k/p}}
\tag{2.2}
$$

where $p = \min\{k-1, 2\}$ and c_k is defined in equation (A.3) in Appendix A. Hence, we construct the statistic

$$
\psi_k = \exp\left(\mu_k\right) - 1.
\tag{2.3}
$$

Trapani (2016) showed that ψ_k diverges to positive infinity under H_0, whereas it drifts to zero under H_A. In order to produce a test statistic which has a well-defined limiting law, ψ_k is randomised by using the following algorithm.

Step 1 Randomly generate an *i.i.d.* $N\left(0,1\right)$ sample of size $R = \left\lfloor T^{1/2}\right\rfloor$, say $\left\{\xi_j^{(k)}\right\}_{j=1}^{R}$, independently across k, and define $\left\{\psi_k^{1/2} \times \xi_j^{(k)}\right\}_{j=1}^{R}$.

Step 2 For $u \in \left\{-\sqrt{2}, \sqrt{2}\right\}$, generate $\zeta_{j,T}^{(k)}\left(u\right) = I\left(\psi_k^{1/2} \times \xi_j^{(k)} \le u\right)$, $1 \le j \le r$.

Step 3 For each u, define

$$
\vartheta_{T,R}^{(k)}\left(u\right) = \frac{2}{\sqrt{R}}\sum_{j=1}^{R}\left[\zeta_{j,T}^{(k)}\left(u\right) - \frac{1}{2}\right],
\tag{2.4}
$$

and finally the test statistic

$$
\Theta_{T,R}^{(k)} = \frac{1}{2}\left[\left(\vartheta_{T,R}^{(k)}\left(-\sqrt{2}\right)\right)^2 + \left(\vartheta_{T,R}^{(k)}\left(\sqrt{2}\right)\right)^2\right].
\tag{2.5}
$$

The limiting distribution of $\Theta_{T,R}^{(k)}$ is in Theorem A.1 in Appendix A; in essence, under the null, $\Theta_{T,R}^{(k)}$ follows a chi-squared distribution with one degree of freedom (henceforth χ_1^2). However, this result is different from a standard limit theorem, and it suffers from a replicability issue which we now proceed to explain. Indeed, under H_0 it holds that

$$
\lim_{\min(T,R)\to\infty} P^*\{\Theta_{T,R}^{(k)} \ge c_\alpha\} = \alpha,
\tag{2.6}
$$

6

conditional on the sample, where c_α is a critical value defined by $P\left(\chi_1^2 \geq c_\alpha\right) = \alpha$. However, the test statistic $\Theta_{T,R}^{(k)}$ is constructed using the randomness $\left\{\xi_j^{(k)}\right\}_{j=1}^R$, which does not vanish asymptotically. As a consequence, different researchers using the same data will obtain different values of $\Theta_{T,R}^{(k)}$ and, therefore, different p-values; indeed, if an infinite number of researchers were to carry out the test, the p-values would follow a uniform distribution on $[0, 1]$. This is a well-known feature of randomised tests (see e.g. the discussion in Horváth and Trapani, 2019).

In order to address the issue mentioned above, we construct a "strong" (i.e., valid almost surely) decision rule which ensure that the decision between H_0 and H_A is not subject to such arbitrariness, and that all researchers will end up having the same outcome. Our decision rule works as follows. Each researcher, instead of computing $\Theta_{T,R}^{(k)}$ just once, will compute the test statistic S times, at each time s using an independent sequence $\left\{\xi_j^{(s)}, 1 \leq j \leq R\right\}$ for $1 \leq s \leq S$, thence defining

$$Q^{(k)}(\alpha) = S^{-1} \sum_{s=1}^S I\left[\Theta_{T,R,s}^{(k)} \leq c_\alpha\right], \tag{2.7}$$

where $\Theta_{T,R,s}^{(k)}$ is the test statistic computed according to the algorithm above using the artificial sample $\left\{\xi_j^{(s)}, 1 \leq j \leq R\right\}$. The function $Q^{(k)}(\alpha)$ is related to the "fuzzy confidence interval" discussed in equation (1.1b) in Geyer and Meeden (2005). We note (heuristically) that an immediate consequence of Theorem A.1 is

$$\begin{aligned}
\lim_{\min(T,R,S)\to\infty} P^*\{Q^{(k)}(\alpha) = 1 - \alpha\} = 1 \quad &\text{under } H_0 \\
\lim_{\min(T,R,S)\to\infty} P^*\{Q^{(k)}(\alpha) = 0\} = 1 \quad &\text{under } H_A
\end{aligned} \tag{2.8}$$

This indicates that, as $S \to \infty$, $Q^{(k)}(\alpha)$ has been "de-randomised" - that is, the randomness added by the researcher has been washed out, and the conclusions drawn from a test based on $Q^{(k)}(\alpha)$ are exactly the same across all researchers. We formalise the properties of $Q^{(k)}(\alpha)$ in Theorem A.2 in Appendix A. Based on the results in Theorem A.2, a decision rule in favour of H_0 can be based on

$$Q^{(k)}(\alpha) \geq (1 - \alpha) - \frac{\sqrt{\alpha(1-\alpha)}}{f(S)}, \tag{2.9}$$

7

for all sequences $f(S) \to \infty$ such that $f(S) = o(S^{1/2})$. In the empirics section, we discuss the choice of $f(S)$ and the robustness of $Q^{(k)}(\alpha)$ to its choice.

2.2. Assessing the impact of infinite moments in risk management

We consider a representative trader with unlimited capital, who wants to calculate her VaR measure at each point in time. Without loss of generality, each trading day t is divided in τ equidistant intraday subintervals. The observed prices at day t are denoted as P_{t_j}, for $j = 1, 2, ..., \tau$, with sample frequency defined as $m = \tau^{-1}$. We define daily log-returns as $y_t = logP_{t_\tau} - logP_{(t-1)_\tau}$, and intraday log-returns as $y_{t_j} = logP_{t_j} - logP_{t_{j-1}}$.

The VaR for a long trading position at $(1-p)$ level of confidence, at sampling (trading) frequency m, is denoted as $VaR^{(m)}_{(1-p)}$, defined such that $P(y_{t_j} \leq VaR^{(m)}_{(1-p)}) = p$. The $VaR^{(m)}_{(1-p)}$ is computed non-parametrically as the p-quantile of the intraday log-returns at sampling frequency m: $VaR^{(m)}_{(1-p)} = f_p(\{y_{t_j}\}_{j=1,...,\tau}^{t=1,...,T})$.[4] We measure the potential losses conditional to a VaR violation (i.e. the losses that occur when the returns are lower than the VaR measure) by constructing an evaluation function, $l_{t_j}^{(m)}$ that measures the absolute distance between actual returns, y_{t_j}, and the VaR measure, i.e. the potential loss $(l_{t_j}^{(m)})$:

$$l_{t_j}^{(m)} = \begin{cases} |y_{t_j} - VaR^{(m)}_{(1-p)}| & \text{if } y_{t_j} < VaR^{(m)}_{(1-p)} \\ 0 & \text{otherwise.} \end{cases} \tag{2.10}$$

We note that the expected shortfall, recently proposed as an alternative risk measure, is the expectation of the potential loss $(\mathbb{E}(l_{t_j}^{(m)}))$, given that the VaR violation is present.

The total potential losses over the sample period are computed as $L^{(m)} = \sum_{t=1}^{T} \sum_{j=1}^{\tau} l_{t_j}^{(m)}$. To allow comparison across the different sampling frequencies we also compute the daily adjusted losses per VaR violation as $\bar{L}^{(m)} = 1361(Nm)^{-1}L^{(m)}$, for $N = \sum_{t=1}^{T} \sum_{j=1}^{\tau} I_{t_j}^{(m)}$, where:

---

[4]The VaR of intraday log-returns y_{t_j} for a short trading position at $(1-p)$ level of confidence at sampling frequency m is $P(y_{t_j} \geq VaR^{(m)}_{(1-p)}) = (1-p)$.

$$I_{t_j}^{(m)} = \begin{cases} 1 & \text{if } y_{t_j} < VaR_{(1-p)}^{(m)} \\ 0 & \text{otherwise.} \end{cases} \qquad (2.11)$$

We multiply the number of violations by the daily adjustment, $1361/m$, where 1361 reflects the 1-minute observations per day that the market is open.

3. Empirical findings from actual data of three currency pairs

In this section, we carry out an empirical exercise, where we *(i)* check whether our data have heavy tails or not (by testing for the finiteness of up to the fourth moment); and *(ii)* evaluate the potential losses when using a strategy that fails to acknowledge that higher order moments are infinite. We find that, when considering intraday frequency data, higher order moments such as the kurtosis are infinite; and that potential losses tend, in such cases, to be much higher than anticipated.

3.1. Data description

We use 1-minute data of the front-month futures contracts, as well as, the spot prices, for the EUR/USD, GBP/USD and CAD/USD exchange rates, obtained from TickData and HistData, respectively. The period of the study spans from January 3, 2000 to August 5, 2015 for the futures data, whereas, due to data availability issues, the sample period for the spot prices runs from January 3, 2005 to August 5, 2015. We focus on a sample of the G10 exchange rate market as it is considered the deepest continuously trading market in the world, so that we do not have to take into consideration significant data alterations. The choice of the specific currency pairs is justified by the fact that *(i)* they are among the most liquid, and *(ii)* they represent the most heavily traded exchange rate for financial transactions. Our sample consists of $3,990$ trading days, which contain more than 25 million 1-minute data in total.

Descriptive statistics - for the currency pairs' spot and futures returns for sampling (trad-

ing) frequencies from 1-minute to 1-day - are summarised in Table B.1 in Appendix B. We note that volatility is falling linearly as the sampling frequency is increasing. By contrast, the third moment (skewness) does not change materially from symmetry at the different frequencies. More importantly, the fourth moment (kurtosis) shows the well documented leptokurtosis, which increases dramatically as the sampling frequency increases. This is particularly evident for the futures price returns, which suggests that investors in the futures market are exposed to greater tail risk. Of course, the magnitude of kurtosis at the higher frequencies differs among the different crosses, with the higher values to be observed in the EUR/USD.

3.2. Testing for the finiteness of higher order moments

We start our analysis with the results on the finiteness of moments in Tables 1 and 2.[5] When computing (2.9), we used the same specifications as in the paper by Trapani (2016) - namely, we set $R = \lfloor T^{1/2} \rfloor$ (note that T is a much larger number than in the simulations considered in Trapani (2016), so R is likely to be much larger than needed). Consistently with Theorem A.2, we chose $S = 2,000$, which is essentially the same order of magnitude as R for all cases considered; we would like to point out that we tried to vary S, but results are virtually unchanged. Finally, in the computation of the threshold for $Q^{(k)}(\alpha)$, we use $f(S) = S^{1/4}$; we note that functions like $f(S) = S^a$, for $0 < a < \frac{1}{2}$, are in principle all acceptable. We experimented with different functional forms for $f(S)$, using e.g. $f(S) = S^{1/3}$ and $f(S) = S^{1/5}$, but results are exactly the same, which illustrates the robustness of our procedure to this specification.

[Insert Tables 1 and 2 around here]

The results in Tables 1 and 2 show that the second moment is finite across all currencies

---

[5]We have also considered lower frequencies than the daily (e.g. weekly, biweekly and so on) and the results show that all moments continue to be finite. These unreported results are available from the authors upon request.

and sampling frequencies (for both spot and futures returns), whereas skewness seems to exist in most cases, with the main exceptions being the 1m-20m frequencies for the EUR/USD and GBP/USD futures. More importantly, though, for all intraday sampling frequencies across the three currency pairs (either in their futures or spot returns), the null hypotheses of infinite fourth moment cannot be rejected, lending preliminary support to the *superkurtosis* phenomenon. On the other other hand, moving to lower sampling frequencies, i.e. daily, we find evidence that all moments are finite.

3.3. The impact of the infinity of moments in intraday returns

The results presented in Tables 1 and 2 seem to suggest that risk management tools, such as the VaR or ES, that are used by implicitly assuming finite moments, might be inappropriate to assess the true underlining risk of loss in the ultra-high frequencies. To ascertain this, we consider a scenario where traders assume that high order moments are finite at the intraday frequencies. Under this scenario, we calculate the potential losses ($L^{(m)}$ and $\bar{L}^{(m)}$), conditional to VaR violation, as shown in Section 2.2 (see Figures 1 and 2, which depict the results for the futures and spot price returns, respectively).

[Insert Figure 1 around here]

In all cases considered in Figure 1, potential losses are decidedly higher for the higher sampling (trading) frequencies, while they decrease rapidly as the sampling (trading) frequency decreases. This holds for both the total potential losses ($L^{(m)}$) and the daily adjusted potential losses ($\bar{L}^{(m)}$). For instance, in the 1-minute trading frequency of the EUR/USD futures prices we observe that a trader would have lost 48 times more capital than anticipated by the VaR, whereas the daily adjusted losses, for the same frequency, are about 25% more. Similar figures are reported for the GBP/USD and CAD/USD futures prices, as well[6].

---

[6]Please note that we have also considered a short position in the currency pairs and the results are qualitatively similar, suggesting that the infinity of the third moment that was exhibited in some frequencies

11

We supplement our analysis by focusing also on the spot prices of the three currency pairs. We do so, since the spot and futures prices are related via covered interest rate parity and thus the empirical findings could be driven by the interest rate differential component. Figure 2 depicts the potential losses and daily adjusted potential losses conditional to VaR violations, using the spot exchange rates. We observe that the potential losses increase exponentially as the trading frequency increases. For instance, the potential losses in all currencies are 30 times larger at the 1-min sampling frequency, suggesting that a trader is anticipated to lose 30 times more capital (or about 25% based on the daily adjusted losses) more than anticipated by the VaR, when she trades on a 1-min frequency. Although the magnitude of the potential losses is lower compared to the futures prices (for the Euro/Dollar futures the potential losses were 48 times higher at the 1-min sampling frequency), we can immediately understand that the main findings observed using the futures prices remain unchanged for the case of spot prices.

[Insert Figure 2 around here]

To elaborate further on our key finding, we proceed with a simple example of the consequence of ignoring the infinity of high-order moments and in particular, the *superkurtosis* phenomenon, by quantifying how much a trader is miscalculating her expected losses. To do so, we assume three representative traders that each have an initial capital of $10,000$. The only difference among the three traders is the choice of trading frequency. Indicatively, we assume that the first trader chooses to trade every minute, the second every 60 minutes and the third trader makes her trades on a daily basis. Furthermore, the traders have an investment horizon equal to our sample period. Each trader calculates her 95% VaR measure and invests the capital that respects the VaR in the foreign exchange market at each point in time. To quantify the miscalculation of the potential losses we proceed as follows. When the trader makes a positive return or a loss that falls within the VaR, then we report this

cannot be blamed for the observed behaviour of the potential losses.

as a zero potential excess loss. However, when the trader suffers a loss greater than the 95%
VaR number then we calculate the excess loss beyond and above the VaR (for the specific
minute, hour or day). We do that for all trading observations of each trader and we then
aggregate these excess losses over the sample period. We do so to quantify the maximum
potential excess losses (rather than the actual losses) of each trader. For brevity, Figure 3
presents only the cumulative potential excess losses for each trader for the EUR/USD futures
market.

[Insert Figure 3 around here]

Figure 3 clearly demonstrates the severity of the issue discussed in this paper. The po-
tential excess losses for 1 minute trader is massively higher compared to the daily trader.
In particular, based on the study period used in this paper, the potential excess loss for
the 1 minute trader reaches the level of almost $600,000$, which means that the trader can
potentially deplete her capital within a very short period of time (in the first 3-months in
our numerical example), showing that VaR is heavily misleading. By contrast, for the daily
trader this amount is about $9,000$, which means that this trader never depletes her capital
and thus VaR is a valid risk management metric in this context.

3.4. Robustness analysis

To complement our empirical analysis based on the actual intraday data of the three cho-
sen currency pairs, we further assess our findings by distinguishing between intraday and
overnight returns, as well as, between the ebb and flow trading periods. Finally, we assess the
validity of our findings using a carry trade strategy where the investor goes long on the high
interest rate and short on the low interest rate currency.

Initially we remove the overnight returns from the intraday returns of our futures prices.
We time stamp our analysis considering as closing times the period between 4:00pm and
5:00pm Chicago time. Thus, we remove the overnight returns (which are defined as the

returns occurring between the closing time of the day and the opening time of the next day) and we re-estimate the potential losses and daily adjusted potential losses. Figure 4 presents our results.

[Insert Figure 4 around here]

Similarly to our previous analysis, we note that removing the overnight returns does not alter our main findings, showing that our results are not driven by the potential price jumps that could be observed when the market is considered closed.

Next, we proceed with an additional robustness check, distinguishing the futures price returns between the ebb and flow transaction periods. The busiest time zones for foreign exchange trading are London and New York. Thus, we isolate the intraday futures returns of our currency pairs for the time period 2:00am to 3:00pm Chicago time, which denote the high trading period and we leave the remaining opening hours as the low trading period. The results are shown in Figures 5 and 6. The results are qualitatively similar to our initial findings from Figure 1.

[Insert Figures 5 and 6 around here]

To complement further our empirical analysis based on actual intraday data, we proceed with a currency carry trade. To do so, we use one of the most popular carry trades, which is going long the Australian Dollar (AUD) and short the Japanese Yen (JPY). As in the previous analysis, Figure 7 suggests that the main findings not only still persist, but they are exacerbated. Using once again the 1-min sampling frequency, we document that the potential losses are more than 60 times higher compared to the amount anticipated by the VaR, which translates into 45% more daily adjusted potential losses.

[Insert Figure 7 around here]

4. Findings from simulated data

Our analysis above shows that the *superkurtosis* phenomenon, i.e. the infinite kurtosis, could be the source of the extreme potential losses as the sampling (trading) frequency increases. However, the actual source of these losses is rather unclear. Thus, to shed light in this respect we now perform an experiment using simulated data, to pin down the most important sources of the association between potential losses and frequency of trading. Specifically, we assess the impact of the sample size on potential losses, showing that as this increases, so do the potential losses. Further, we assess the impact of having heavy tails on the potential losses. We find that sample moments, when population moments are infinite, tend to be much higher than the SLLN would suggest, which we show is particularly true for the sample kurtosis.

4.1. Assessing the impact of the sample size on potential losses

We analyse - via a simulation exercise - the impact of the sample size on potential losses, considering a Gaussian data generating process where we simulate the (log) prices, $\log(P_t)$, for $1 \leq t \leq 10^6$ as

$$\log(P_t) = \log(P_{t-1}) + z_t, \tag{4.1}$$

with $z_t \overset{i.i.d.}{\sim} N(0, 1/h^2)$, and initial price $P_1 = \$1,000$. The total sample is split in $1,000$ trading days with $1,000$ intraday prices. Without any loss of information, the sample $\{P_t\}_{t=1}^{10^6}$ mimics the P_{t_j} for $j = 1, ..., 1,000$ and $t = 1, ..., 1,000$, at sampling (or trading) frequency $m = 10^{-3}$. For example, at 1-minute sampling frequency, or $m = 10^{-3}$, we have $\tau = 1,000$ intraday prices, for $T = 1000$ trading days, at 2-minutes sampling frequency, we have $\tau = 500$ intraday prices, for $T = 1,000$ trading days, and so on.

Figure 8 illustrates the $VaR_{(95\%)}^{(m)}$, the kurtosis of log-returns, $y_{t_j} = \log(P_{t_j}) - \log(P_{t-1_j})$, and the potential losses $L^{(m)}$, $\bar{L}^{(m)}$ for the simulated log-returns. We have set $h = 10$; we note however that, in unreported experiments, very similar results were found when using different values of h. The x-axis presents the trading frequency in minutes, from 1 up to 120 minutes. Without any loss of generality, we assume a long trading position, hence the 95%

15

VaR measure is computed as the 5% quantile point of the empirical distribution of y_{t_j}.[7]

[Insert Figure 8 around here]

The simulated results provide us with an important finding: the potential losses are dependent on the trading frequency, where higher trading frequency leads to higher potential losses, despite the fact that the kurtosis (upper right graph) is around the value of 3 across any trading frequency $m = 1, ..., 120$. So, such finding could simply suggest that the increased potential losses are not related with the effect of *superkurtosis*, but rather they are the artifact output of the effect of number of observations which increases exponentially as the sampling frequency increases.

In order to shed further light on the impact of the sample size, we investigate the analytical form of the total potential losses. The potential loss $L^{(m)}$ is given by

$$L^{(m)} = \sum_{t=1}^{T} \sum_{j=1}^{\tau} \left(|y_{t_j} - VaR_{(1-p)}^{(m)}| \times I_{\{y_{t_j} < VaR_{(1-p)}^{(m)}\}} \right), \tag{4.2}$$

for $I_{\{.\}}$ representing the indicator variable and we compute the expected value of total potential losses, $\mathbb{E}(L^{(m)})$. For our long trading position and under the condition $y_{t_j} < VaR_{(1-p)}^{(m)}$, we have $y_{t_j} < 0$ and $VaR_{(1-p)}^{(m)} < 0$, as well. So, for $y_{t_j} < VaR_{(1-p)}^{(m)}$, we have $|y_{t_j} - VaR_{(1-p)}^{(m)}| = -(y_{t_j} - VaR_{(1-p)}^{(m)})$. Hence:

$$\mathbb{E}(L^{(m)}) = \sum_{t=1}^{T} \sum_{j=1}^{\tau} E \left(|y_{t_j} - VaR_{(1-p)}^{(m)}| \times I_{\{y_{t_j} < VaR_{(1-p)}^{(m)}\}} \right) = -\sum_{t=1}^{T} \sum_{j=1}^{\tau} p\mathbb{E} \left(y_{t_j} - VaR_{(1-p)}^{(m)} | y_{t_j} < VaR_{(1-p)}^{(m)} \right).$$

$$\tag{4.3}$$

Note also that $\mathbb{E}(I_{\{y_{t_j} < VaR_{(1-p)}^{(m)}\}}) = p$, as well as, that $\mathbb{E}(y_{t_j} | y_{t_j} < VaR_{(1-p)}^{(m)}) = ES_{(1-p)}^{(m)}$, and that $\mathbb{E}(VaR_{(1-p)}^{(m)} | y_{t_j} < VaR_{(1-p)}^{(m)}) = VaR_{(1-p)}^{(m)}$. Hence, it follows that

---

[7]For a short trading position, the 95% quantile point of the empirical distribution would have been considered.

$$\mathbb{E}(L^{(m)}) = -T\tau p(ES^{(m)}_{(1-p)} - VaR^{(m)}_{(1-p)}). \tag{4.4}$$

Under the data generated process of eq. 4.1, it is easy to see that,

$$VaR^{(m)}_{(1-p)} = \Phi_{(1-p)}\left(\mathbb{E}(y_{t_j}) = 0, V(y_t) = \left(\sqrt{\frac{m}{h^2}}\right)^2\right) \tag{4.5}$$

and

$$ES^{(m)}_{(1-p)} = -\frac{\sigma}{1-p}\varphi\left(\Phi_{(1-p)}(0,1)\right), \tag{4.6}$$

where $\varphi(\cdot)$ denotes the standard normal probability density function and $\sigma = h^{-1}\sqrt{m}$. Hence, the $VaR^{(m)}_{(1-p)}$ measure equals to the $(1-p)$ percentile point of the inverse cumulative normal distribution with zero mean and $h^{-1}\sqrt{m}$ standard deviation (we would like to bring to the reader's attention that $m = \tau^{-1}$ is the intraday trading frequency).

So, as presented in Figure 9, the total potential losses per trading frequency m are not only affected by the number of observations ($T\tau$, which denotes the effect of size), but also from the distance between the two risk measures; i.e. the expected shortfall and the VaR, i.e. $(ES^{(m)}_{(1-p)} - VaR^{(m)}_{(1-p)})$. Therefore, as the trading frequency increases, (i) the number of trades increases exponentially (see the effect of size in Figure 9), while (ii) the distance between the two risk measures decreases (see the expected shortfall and value-at-risk in Figure 9). Indicatively, some estimates of (4.4) are $\mathbb{E}(L^{(1)}) = 0.02089$ and $\mathbb{E}(L^{(120)}) = 0.00191$, for $ES^{(1)}_{(5\%)} - VaR^{(1)}_{(5\%)} = 4.2E - 7$ and $ES^{(120)}_{(5\%)} - VaR^{(120)}_{(5\%)} = 4.6E - 6$.

[Insert Figure 9 around here]

Thus, both analytical and simulated evidence show that the total potential losses per trading frequency m are affected positively by the number of trades and negatively by the distance between the two risk measures. Having established the aforementioned effects, in

17

the paragraphs that follow, we investigate whether there are any additional effects from the infinity of moments.

4.1.1. Assessing the impact of heavy tails on potential losses

We now turn to investigating the effect of heavy tails on potential losses; in particular, we assess the impact of *superkurtosis*. To this end, we consider a heavy tailed data generating process, as follows:

$$\log(P_t) = \log(P_{t-1}) + z_t, \tag{4.7}$$

for $z_t \overset{i.i.d.}{\sim} t(0, 1/h^2, v)$, for $v \geq 2$ and initial price of $P_1 = \$1,000$. The probability density function for Student t is considered as: $\varphi(0, 1/h^2, v) = \frac{\Gamma(\frac{v+1}{2})}{\Gamma(\frac{v}{2})\sqrt{\frac{\pi v}{h^2}}} \left(1 + \frac{z_t^2 h^2}{v}\right)^{-\frac{v+1}{2}}$.

Figure 10 shows the values of the sample kurtosis and the potential losses $L^{(m)}, \bar{L}^{(m)}$ for the simulated log-returns, from the Student t random walk data generated process under various degrees of freedom, $v = 3, 4, 5, 10, 30, 100$ and $h = 10$; clearly, the population kurtosis does not exist for the first two values.

[Insert Figure 10 around here]

We note that, for the near-Gaussian cases $v = 30$, and 100, the kurtosis remains constant across various values of trading frequency, and, as expected, the potential losses $L^{(m)}$ and $\bar{L}^{(m)}$ are almost identical to those found in the previous section. As is natural to expect, as the degree of freedom v decreases, the sample kurtosis increases; for example, for $v = 10$, the kurtosis of log-returns at 120-minutes trading frequency is around 3.1, whereas for $v = 3$ the kurtosis of log-returns at 120-minutes trading frequency is around 3.6. However, Figure 10 shows a remarkable feature of the sample kurtosis. Heuristically, when $v \leq 4$, the sample kurtosis should pass to infinity as the sample size $T\tau \to \infty$; in particular, the Marcinkiewicz-Zygmund SLLN implies that the sample kurtosis should pass to infinity at a rate given by

18

(modulo some slowly varying sequence) $O\left((T\tau)^{\frac{4-v}{v}}\right)$. For example, when $v = 3$, the sample kurtosis should diverge to infinity as fast as (approximately) $O\left((T\tau)^{1/3}\right)$. Based on these heuristic considerations, when e.g. $v = 3$, one could expect the sample kurtosis for the 1-minute trading frequency to be larger by a factor $120^{1/3}$ than the sample kurtosis calculated for the 120-minutes trading frequency, keeping T constant. On the contrary, from Figure 10, it is apparent that the sample kurtosis is larger than the theory would predict. For example, for $v = 3$, the 1-minute sampling frequency log-returns have kurtosis of 96, which is approximately 26 times as much as in the 120-minute sampling frequency case, whereas the theory would predict an increase of approximately 5 times only.

Turning now to the relationship between kurtosis and potential losses at the highest trading frequency of 1-minute, we document that a kurtosis of 4 (as derived for $v = 10$ degrees of freedom) implies potential losses of $L^{(1)} = 27.8$ and $\bar{L}^{(1)} = 0.80$, whereas a kurtosis of 96 (as derived for $v = 3$) increases the potential losses to $L^{(1)} = 75.8$ and $\bar{L}^{(1)} = 2.18$.

To segregate the effect of the mechanically increasing sample size from this of the *superkurtosis*, we normalize the potential loss measure so to remove the effect of the former. To do so, we compute the ratio of the potential losses across sampling frequencies from the data generated process $\log(P_t) = \log(P_{t-1}) + z_t$, for $z_t \overset{i.i.d.}{\sim} t(0, 1/h^2, v)$, at different degrees of freedom. Indicatively, Figure 11 presents the ratio of potential losses for $v = 3$ and $v = 30$ degrees of freedom. For example, at 1-minute sampling frequency the $L^{(1)}$ for $v = 3$ is 75.43 and for $v = 30$ is 23.49, hence the ratio, as presented in Figure 11, is 3.21 times. In other words, *superkurtosis* leads to 3.3 times higher potential losses at 1-minute sampling frequency. This finding holds across all sampling frequencies, however, it is evident that as the sampling frequency increases, the effect of *superkurtosis* is magnified exponentially.

[Insert Figure 11 around here]

Both simulated and analytical results strengthen our findings, from the real data, that the potential losses are dependent on the trading frequency, where higher trading frequency leads

19

to higher potential losses. Most importantly, though, we observe the effect of *superkurtosis*, which is also evident in the real data, to influence radically the potential losses. Put differently, the shape of the potential losses from the simulated data do resemble those of the actual data. Thus, as the sampling (trading) frequency increases, the effect of *superkurtosis* becomes more material and the potential losses increase substantially.

Finally, we would like to highlight that we have further experimented with the previous simulation for $P_1 = 1$ in order to mimic the exchange rate values, as well as, using a conditionally heteroscedastic data generating process and the results remain robust.[8]

5. Discussion and conclusions

It is common practice for risk metrics users to assume that the moments of asset returns are finite, and to use this assumption to capture the potential losses from asset trading, using metrics such as the VaR or ES. Whilst this assumption appears to be correct for daily frequencies, it is not clear whether this also entails that it holds for higher, intraday frequencies. Further, if this assumption fails to hold, it is not clear what the likely consequences are. On the other hand, whilst computing the VaR under non Gaussian assumptions is perfectly possible, existing methodologies require several assumptions which, if not satisfied, may make calculations unreliable. Hence, it is important to have a methodology to verify whether the assumption of finite higher order moments is adequate.

In this paper, we make two contributions. Firstly, we develop a (replicable) methodology to assess whether the moments of intraday data are finite or not. Secondly, we thoroughly assess the potential losses arising from intraday trading, when a risk management metric, such as VaR or ES, is used under the implicit assumption that the higher order moments of asset returns are finite. Using both real data and a simulation exercise, we (unsurprisingly) find that, when daily trading is implemented, VaR estimates work as expected, with potential losses being in line with what the theory predicts. Conversely, results are far from standard when high frequency, intraday trading is considered. In this case, the potential losses are much

---

[8]Results are not reported in this paper for the sake of brevity, and they are available upon request.

larger than what the theory predicts. We show that there are two concurring features that can explain our findings. Firstly, the sample size itself: as the sampling frequency increases, so does the number of datapoints; hence, our results show that this (obviously) increases the potential losses. Secondly and more importantly, intraday data are more likely to have heavy tails. In our simulations, we show that the sample kurtosis computed using datasets with infinite fourth moment tends to be much higher than what the theory would predict, which in turn, further increases the potential losses. We call this discrepancy between the theoretical behaviour and the actual magnitude of the sample kurtosis *superkurtosis*, and we argue that it is one component of the heavy potential losses which, as a stylised fact, are encountered when trading at intraday frequency under the (implicit in the use of VaR or ES) assumption that high order moments are finite when, in fact, they are infinite.

Our findings entail that employing traditional risk measures for market participants who engage in intraday trading imposes serious threats to the stability of financial markets, given that capital ratios may be severely underestimated. Indeed, based on our analysis, it follows that the hidden risks from intraday trading in the foreign exchange market alone in the financial system are immense, and minimum capital requirement must be substantially increased in such higher trading frequencies, so that risk metrics like VaR or ES match the central bank's capital adequacy preset levels for financial stability reasons.

Currently, the importance of the frequency of trading is typically underplayed. For instance, the Fundamental Review of the Trading Book framework recently finalised by the ECB[9] emphasizes the importance of including risk factors such as the ES in an institution's risk metrics, but it does not offer any guidance as to how a risk factor might change in value when trading takes place at extremely high frequency or how the fair value of a trading asset might be impacted by the frequency of trading. Perhaps more importantly, our findings also have implications for the development of the financial institutions risk assessments metrics set by the Bank for International Settlements (BIS). Appropriate risk measurement is key to the

---

[9]https://www.eba.europa.eu/regulation-and-policy/market-risk/draft-technical-standards-on-the-ima-under-the-frtb

assessment of both firm-specific risk and of aggregate risk, independently of the leverage used by financial institutions. In this sense, if capital requirements, which are designed to mitigate the losses incurred in extreme events, are mis-measured, then they do not solve the underlying problem that arises from a potential underestimation of actual risks that arise from intraday trading. For instance, in the most recent report of BIS for the minimum capital requirements for market risk, in 2019,[10] the severity of intraday trading is acknowledged, noting that banks "are expected to maintain strict risk management systems to ensure that intraday exposures are not excessive" (p.13) - yet maintaining the suggestion that risk metrics, such as ES, should be computed on a daily basis.

The main purpose of this paper is to highlight the stylised fact that intraday trading is based on data with infinite high order moments, and that this invalidates the standard VaR and ES metrics. However, our results also have clear policy implications. Indeed, an immediate conclusion from our findings is that central banks, and banking supervisory authorities, should make use of more appropriate risk metrics that reflect the presence of *superkurtosis*. Several alternatives could be proposed to the classical VaR. For example, a naive, but arguably robust, methodology could be based on multiplying the standard, "Gaussian" estimate of a risk metric by a factor K to take account of the increased trading frequency and of its impact of superkurtosis. Such a factor could be calibrated e.g. by simulation, based on the sample moments of the data at hand. An alternative, more classical, approach could be based on choosing a flexible family of distributions (e.g., the Generalised Pareto Distribution), and using the quantiles thereof instead of the quantiles of the Gaussian distribution. The choice of an appropriate parametric form, in such a case, would be of pivotal importance, as well as the development of a robust estimator. Having a correct measurement of risk metrics is bound to enhance the effectiveness of the macroprudential policies (such as the countercyclical capital buffers and minimum capital requirements), by reducing the vulnerabilities of the financial system, and thus, leading to higher financial stability.

Now more than ever, the use of the correct high frequency risk metrics is of paramount

---

[10]https://www.bis.org/bcbs/publ/d457.pdf

importance, given the ultra-fast emergence of new assets that reflect no economic fundamentals but are heavily traded by market participants, like cryptocurrency perpetual futures, imposing real risks at the very heart of the financial system. The important issues mentioned above are under investigation by the authors.

Acknowledgements

References

Beddington, J., C. Furse, P. Bond, D. Cliff, C. Goodhart, K. Houstoun, O. Linton, and J.-P. Zigrand (2012). Foresight: the future of computer trading in financial markets: final project report.

Bradley, B. O. and M. S. Taqqu (2003). Financial risk and heavy tails. In *Handbook of heavy tailed distributions in finance*, pp. 35–103. North-Holland.

Brush, S., T. Schoenberg, and S. Ring (2015). How a mystery trader with an algorithm may have caused the flash crash. *Bloomberg News 22*.

Geyer, C. J. and G. D. Meeden (2005). Fuzzy and randomized confidence intervals and p-values. *Statistical Science*, 358–366.

Horváth, L. and L. Trapani (2019). Testing for randomness in a random coefficient autoregression model. *Journal of Econometrics 209*(2), 338–352.

Kirilenko, A., A. S. Kyle, M. Samadi, and T. Tuzun (2017). The flash crash: High-frequency trading in an electronic market. *The Journal of Finance 72*(3), 967–998.

Kirilenko, A. A. and A. W. Lo (2013). Moore's law versus Murphy's law: Algorithmic trading and its discontents. *Journal of Economic Perspectives 27*(2), 51–72.

Manganelli, S. and R. F. Engle (2001). Value at risk models in finance. Technical report.

Manhire, J. (2018). Measuring black swans in financial markets. *Journal of Mathematical Finance 8*(1), 227–239.

Michel, R. (1976). Nonuniform central limit bounds with applications to probabilities of deviations. *The Annals of Probability*, 102–106.

Trapani, L. (2016). Testing for (in) finite moments. *Journal of Econometrics 191*(1), 57–68.

Yadav, Y. (2015). How algorithmic trading undermines efficiency in capital markets. *Vanderbilt Law Review 68*, 1607.

TABLE 1

Tests for the finiteness of moments for the futures currency pairs at different sampling (trading) frequencies

Frequency	**Size**	*St.Dev.*		*Skewness*		*Kurtosis*	
		St. Dev.	$Q^{(2)}(\alpha)$	*Skewness*	$Q^{(3)}(\alpha)$	*Kurtosis*	$Q^{(4)}(\alpha)$
			EUR/USD futures				
1m	$5,350,727$	1.88×10^{-4}	0.000	1.806	0.948^*	729.97	0.938^*
2m	$2,675,321$	2.63×10^{-4}	0.000	1.396	0.948^*	395.10	0.941^*
5m	$1,070,147$	4.07×10^{-4}	0.000	0.799	0.953^*	161.38	0.957^*
10m	$535,031$	5.69×10^{-4}	0.000	0.545	0.938^*	85.43	0.939
15m	$356,717$	6.92×10^{-4}	0.000	0.439	0.946^*	62.34	0.942^*
20m	$269,462$	7.94×10^{-4}	0.000	0.469	0.937^*	52.64	0.941^*
30m	$178,316$	9.70×10^{-4}	0.000	0.304	0.902	36.85	0.948^*
60m	$95,138$	13.28×10^{-4}	0.000	0.271	0.820	24.67	0.937^*
daily	$3,990$	64.48×10^{-4}	0.000	0.033	0.000	4.33	0.000
			GBP/USD futures				
		St. Dev.	$Q^{(2)}(\alpha)$	*Skewness*	$Q^{(3)}(\alpha)$	*Kurtosis*	$Q^{(4)}(\alpha)$
1m	$5,142,433$	1.78×10^{-4}	0.000	-0.487	0.948^*	269.39	0.947^*
2m	$2,571,564$	2.12×10^{-4}	0.000	-0.500	0.945^*	119.22	0.940^*
5m	$1,029,113$	3.16×10^{-4}	0.000	-0.422	0.958^*	85.45	0.944^*
10m	$514,904$	4.42×10^{-4}	0.000	-0.364	0.926^*	61.41	0.944^*
15m	$343,557$	5.29×10^{-4}	0.000	-0.348	0.905	36.53	0.942^*
20m	$257,800$	6.16×10^{-4}	0.000	-0.345	0.929^*	41.92	0.940^*
30m	$172,128$	7.44×10^{-4}	0.000	-0.317	0.878	27.83	0.946^*
60m	$89,664$	10.14×10^{-4}	0.000	-0.288	0.729	19.71	0.947^*
daily	$3,990$	56.79×10^{-4}	0.000	-0.321	0.000	5.33	0.000
			CAD/USD futures				
		St. Dev.	$Q^{(2)}(\alpha)$	*Skewness*	$Q^{(3)}(\alpha)$	*Kurtosis*	$Q^{(4)}(\alpha)$
1m	$5,142,433$	1.87×10^{-4}	0.000	0.116	0.942^*	103.30	0.947^*
2m	$2,571,564$	2.57×10^{-4}	0.000	0.067	0.927^*	64.32	0.939^*
5m	$1,029,114$	3.96×10^{-4}	0.000	0.029	0.903	39.46	0.945^*
10m	$514,904$	5.51×10^{-4}	0.000	0.049	0.860	29.89	0.944^*
15m	$343,561$	6.64×10^{-4}	0.000	-0.035	0.801	24.33	0.952^*
20m	$257,800$	7.63×10^{-4}	0.000	0.067	0.786	22.01	0.951^*
30m	$172,128$	9.24×10^{-4}	0.000	0.021	0.717	19.25	0.940^*
60m	$89,664$	12.31×10^{-4}	0.000	0.192	0.686	17.48	0.945^*
daily	$3,990$	58.10×10^{-4}	0.000	-0.142	0.000	6.01	0.000

For each currency, we report the value of the relevant descriptive statistic, and the value of the function $Q^{(k)}(\alpha)$ as defined in equation (2.7). The asterisks next to each value of $Q^{(k)}(\alpha)$ indicate that $Q^{(k)}(\alpha)$ exceeds the threshold defined in (2.9). In turn, this entails that the null that the corresponding, k-th absolute moment is infinite is *not rejected* at nominal level α, thus indicating that the relevant moment is infinite.

TABLE 2
Tests the finiteness of moments for the spot currency pairs at different sampling (trading) frequencies

Frequency	Size	St.Dev.		Skewness		Kurtosis	

		EUR/USD spot					
		St. Dev.	$Q^{(2)}(\alpha)$	*Skewness*	$Q^{(3)}(\alpha)$	*Kurtosis*	$Q^{(4)}(\alpha)$
1m	$3,814,542$	1.80×10^{-4}	0.000	0.337	0.917*	79.58	0.941*
2m	$1,907,174$	2.55×10^{-4}	0.000	0.117	0.920*	71.02	0.941*
5m	$762,817$	3.97×10^{-4}	0.000	0.155	0.880	45.01	0.953*
10m	$381,417$	5.55×10^{-4}	0.000	0.071	0.738	26.34	0.953*
15m	$254,275$	6.78×10^{-4}	0.000	0.353	0.818	30.59	0.941*
20m	$190,704$	7.78×10^{-4}	0.000	-0.001	0.622	20.03	0.953*
30m	$127,134$	9.51×10^{-4}	0.000	0.173	0.619	20.65	0.946*
60m	$63,564$	13.35×10^{-4}	0.000	0.047	0.350	13.93	0.935*
daily	$2,662$	63.12×10^{-4}	0.000	0.198	0.002	6.55	0.004

		GBP/USD spot					
		St. Dev.	$Q^{(2)}(\alpha)$	*Skewness*	$Q^{(3)}(\alpha)$	*Kurtosis*	$Q^{(4)}(\alpha)$
1m	$3,791,546$	1.74×10^{-4}	0.000	-0.025	0.892	46.44	0.941*
2m	$1,895,673$	2.47×10^{-4}	0.000	-0.088	0.913	48.42	0.945*
5m	$758,224$	3.86×10^{-4}	0.000	-0.096	0.868	32.66	0.944*
10m	$379,114$	5.41×10^{-4}	0.000	-0.107	0.781	25.23	0.951*
15m	$252,740$	6.55×10^{-4}	0.000	-0.075	0.707	21.23	0.949*
20m	$189,553$	7.57×10^{-4}	0.000	-0.129	0.776	24.21	0.955*
30m	$126,366$	9.18×10^{-4}	0.000	-0.056	0.601	17.84	0.942*
60m	$63,180$	12.91×10^{-4}	0.000	-0.113	0.524	16.15	0.940*
daily	$2,666$	60.99×10^{-4}	0.000	0.357	0.000	8.12	0.205

|		*CAD/USD spot*					
		St. Dev.	$Q^{(2)}(\alpha)$	*Skewness*	$Q^{(3)}(\alpha)$	*Kurtosis*	$Q^{(4)}(\alpha)$
1m	$3,416,089$	1.97×10^{-4}	0.000	0.049	0.856	40.32	0.950*
2m	$1,707,811$	2.77×10^{-4}	0.000	-0.045	0.855	40.25	0.954*
5m	$683,011$	4.32×10^{-4}	0.000	-0.033	0.699	24.17	0.948*
10m	$341,507$	6.00×10^{-4}	0.000	-0.079	0.562	19.89	0.944*
15m	$227,669$	7.34×10^{-4}	0.000	-0.002	0.533	18.88	0.948*
20m	$170,749$	8.41×10^{-4}	0.000	-0.038	0.454	16.45	0.946*
30m	$113,829$	10.26×10^{-4}	0.000	0.067	0.400	15.13	0.935*
60m	$56,911$	14.35×10^{-4}	0.000	0.044	0.337	14.50	0.934*
daily	$2,686$	65.76×10^{-4}	0.000	0.002	0.000	6.40	0.003

The numbers in the table have the same meaning as in Table 1.

Fig 1: Trader's potential capital losses, on the three futures exchange rates, above the anticipated losses from the VaR measure.
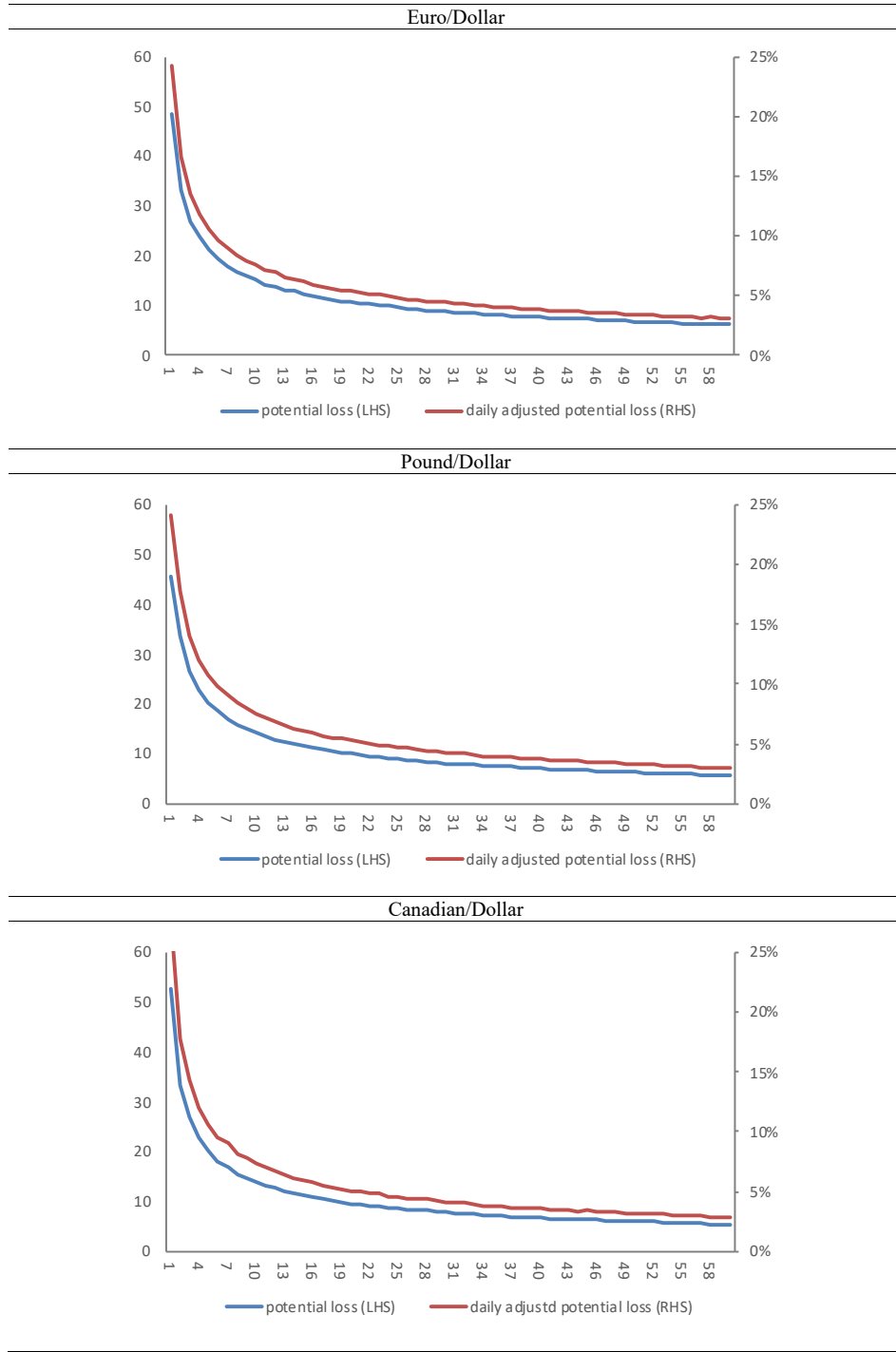
Euro/Dollar

Pound/Dollar

Canadian/Dollar

Note: The x-axis denotes the m=1,...,60 minute intraday sampling (trading) frequencies. The values in the y-axis refer to number of times, whereas in the z-axis refers to percentages.

Fig 2: Trader's potential capital losses, on the three spot exchange rates, above the anticipated losses from the VaR measure.
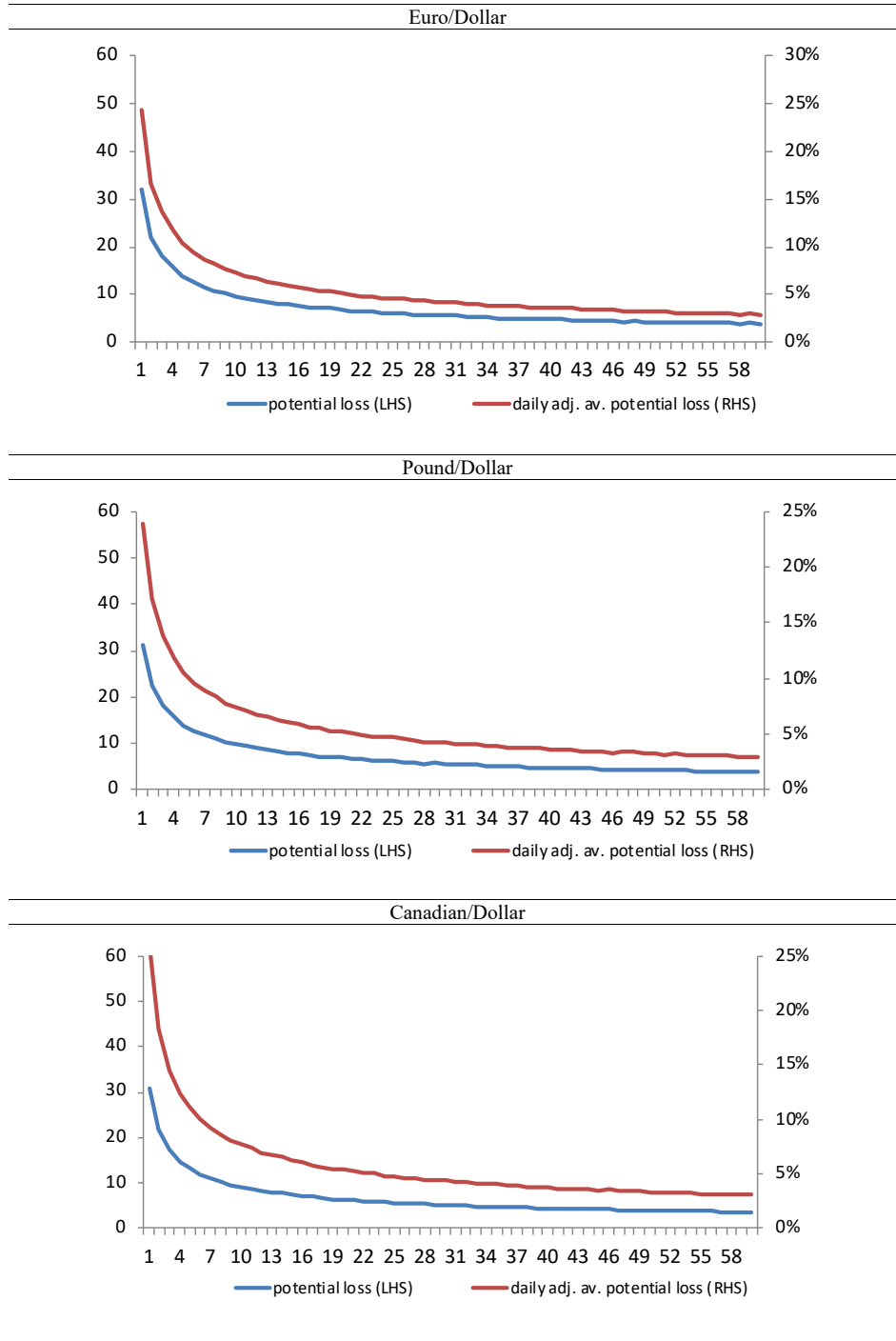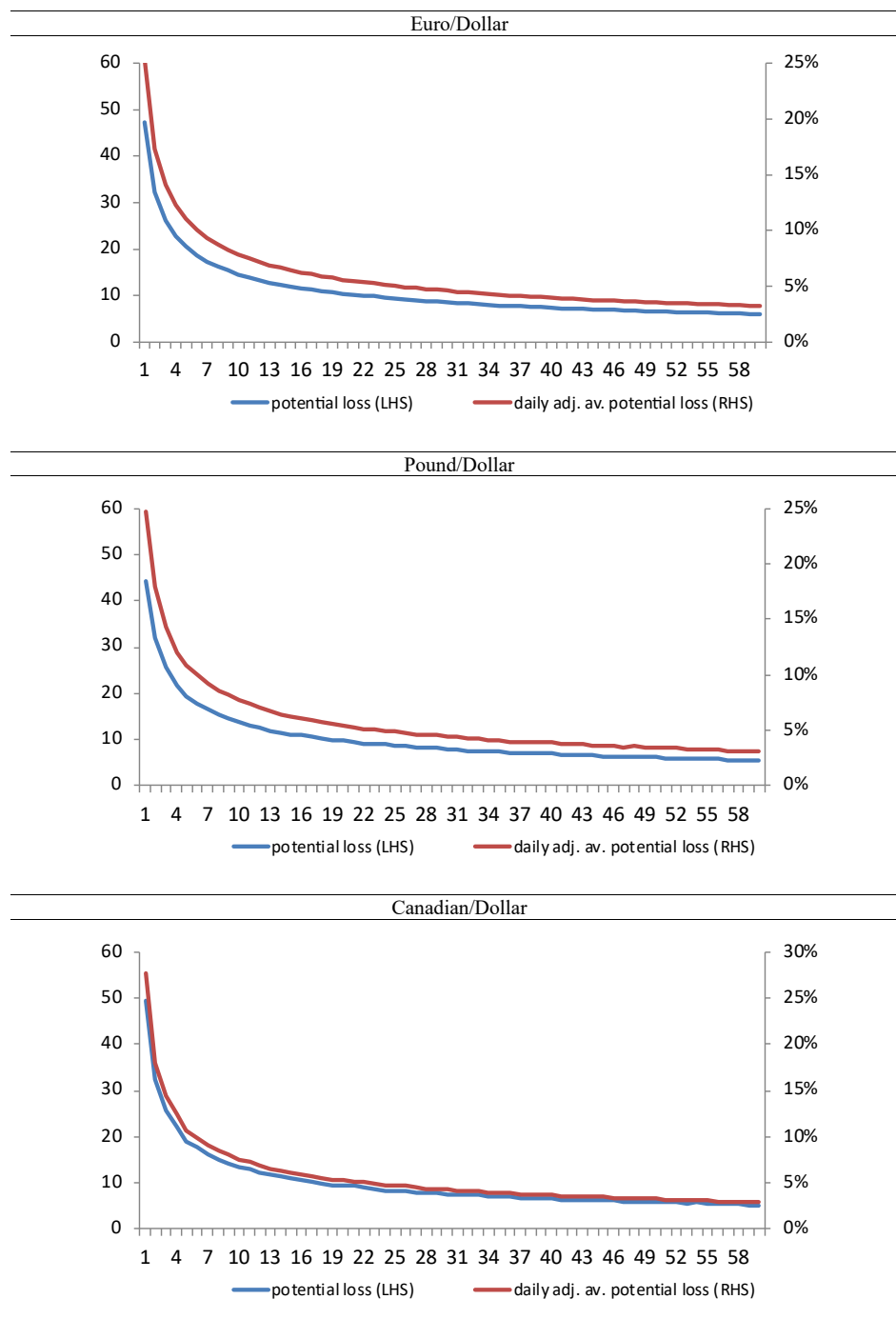

Euro/Dollar

Pound/Dollar

Canadian/Dollar

Note: The x-axis denotes the $m=1,...,60$ minute intraday sampling (trading) frequencies. The values in the y-axis refer to number of times, whereas in the z-axis refers to percentages.

Fig 3: Traders' potential capital losses in $ terms, on the EUR/USD futures exchange rate, above the anticipated losses from the 95% VaR.
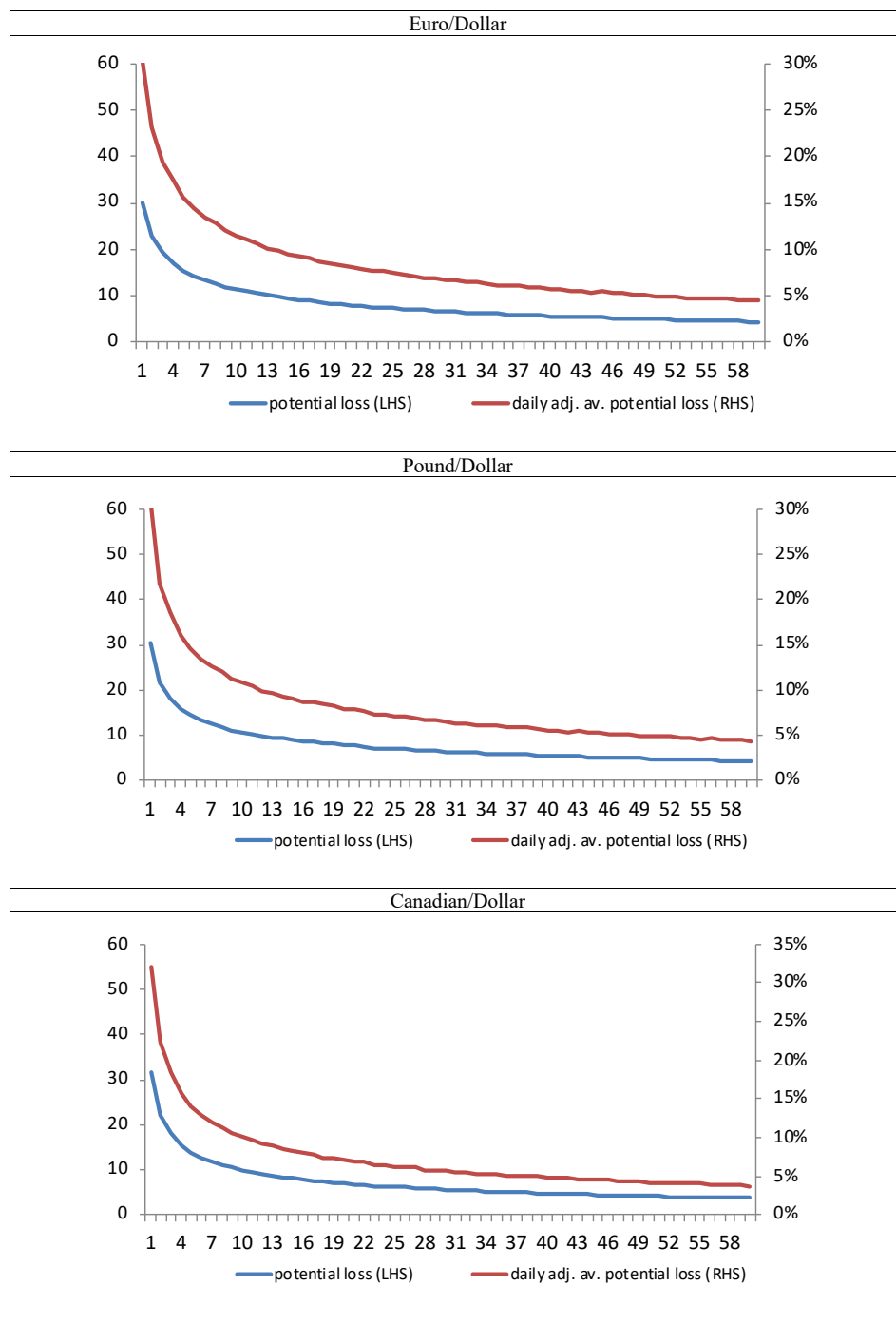

Note: The figure shows the potential losses that can be suffered from three representative traders of the EUR/USD futures prices. From the top panel to the bottom, we show the cumulative potential losses for the 1 minute trader, the 60 minute trader and the daily trader. The y-axis denotes the amount of potential excess losses in $. The values in the x-axes refer to number observations, over the sample period, for the 1 minute trader, 60 minutes trader and the daily trader.

Fig 4: Trader's potential capital losses, on the three futures exchange rates (excluding overnight returns), above the anticipated losses from the VaR measure.

Euro/Dollar

Pound/Dollar

Canadian/Dollar

Note: The x-axis denotes the $m=1,...,60$ minute intraday sampling (trading) frequencies. The values in the y-axis refer to number of times, whereas in the z-axis refers to percentages.
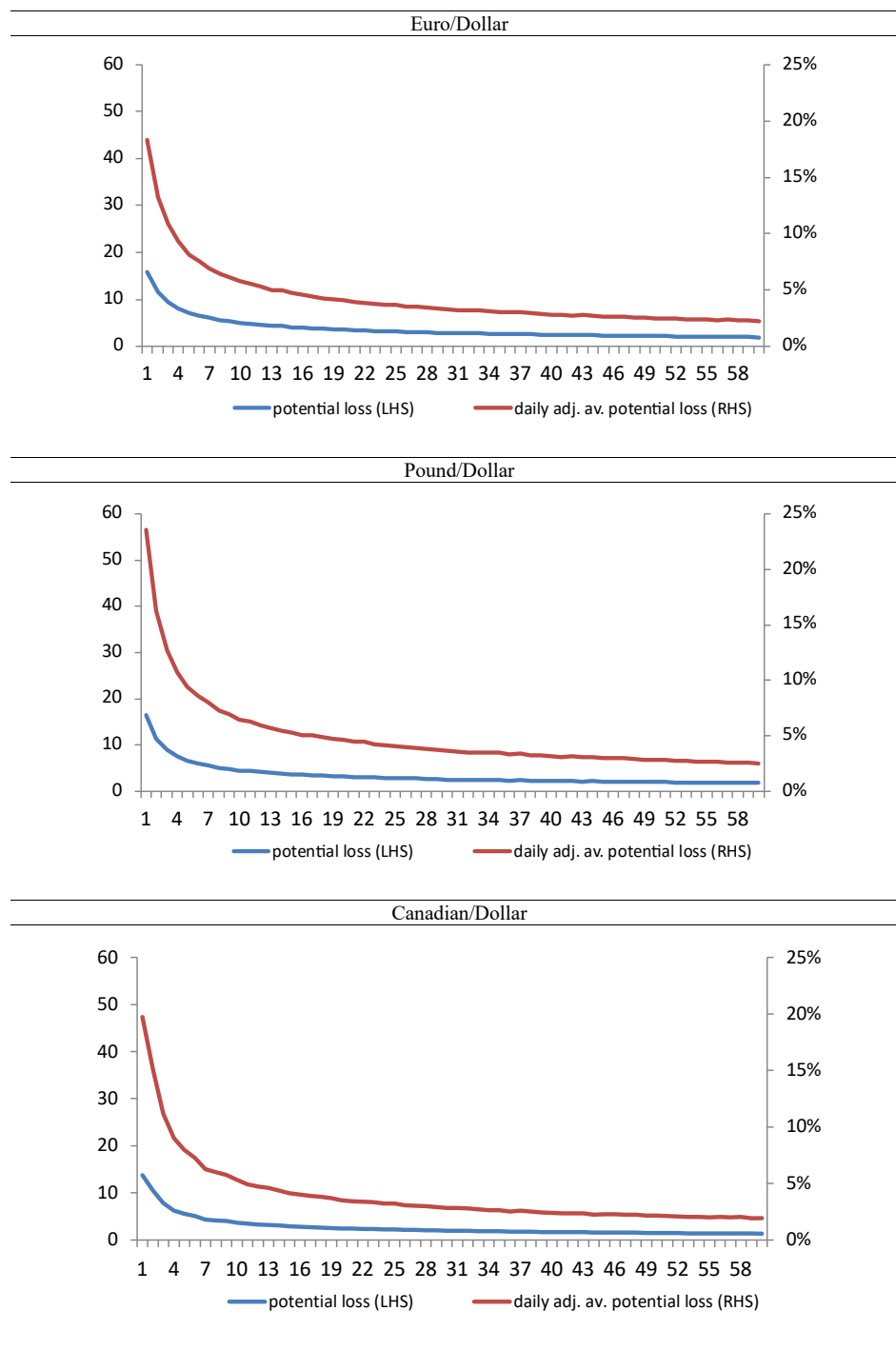
Fig 5: Trader's potential capital losses, on the three futures exchange rates (low transaction period), above the anticipated losses from the VaR measure.

Euro/Dollar

— potential loss (LHS)   — daily adj. av. potential loss (RHS)

Pound/Dollar

— potential loss (LHS)   — daily adj. av. potential loss (RHS)

Canadian/Dollar

— potential loss (LHS)   — daily adj. av. potential loss (RHS)

Note: The x-axis denotes the $m=1,...,60$ minute intraday sampling (trading) frequencies. The values in the y-axis refer to number of times, whereas in the z-axis refers to percentages.
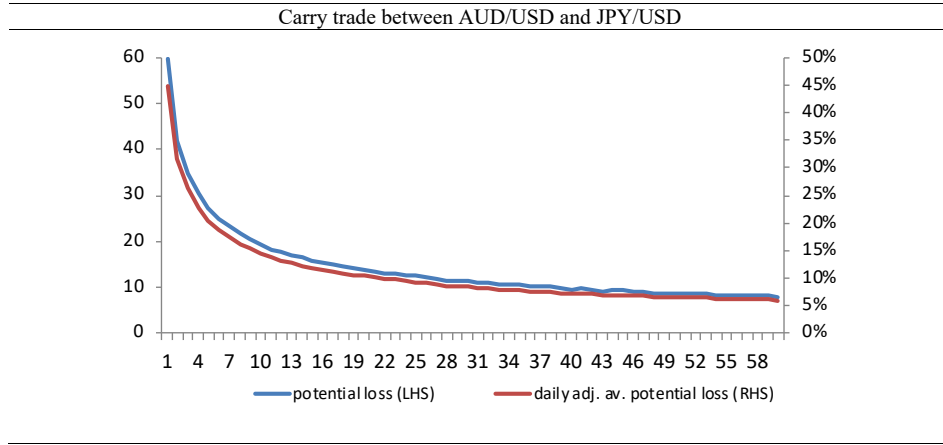
Fig 6: Trader's potential capital losses, on the three futures exchange rates (high transaction period), above the anticipated losses from the VaR measure.

Fig 7: Trader's potential capital losses, on the AUD/JPY carry trade, above the anticipated losses from the VaR measure.

Carry trade between AUD/USD and JPY/USD

potential loss (LHS) — daily adj. av. potential loss (RHS)
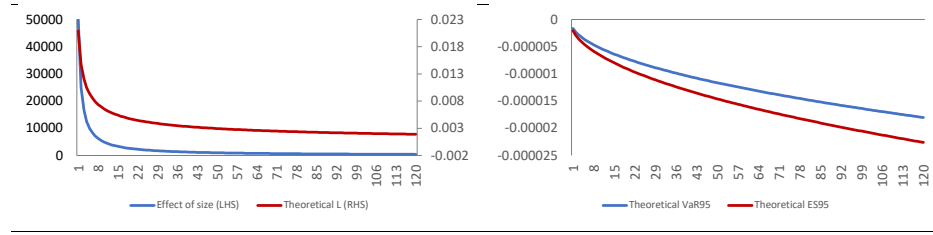
Note: The x-axis denotes the m=1,...,60 minute intraday sampling (trading) frequencies. The values in the y-axis refer to number of times, whereas in the z-axis refers to percentages.

Fig 8: The Value-at-Risk, kurtosis and potential losses for the random walk data generated process.
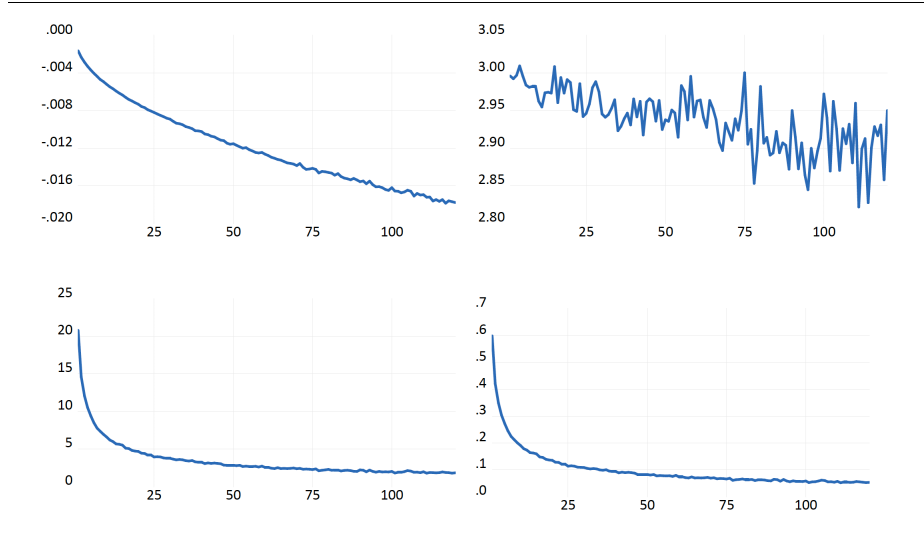

Note: The $VaR_{(95\%)}^{(m)}$ (upper left), the kurtosis of y_t (upper right) and the potential losses $L^{(m)}$ (lower left), $\bar{L}^{(m)}$ (lower right) for the simulated log-returns $y_{t_j} = log(P_t/P_{t-1})$, for $\log(P_t) = \log(P_{t-1}) + z_t$, $z_t \overset{i.i.d.}{\sim} N(0, 1/h^2)$, $P_1 = \$1,000$ and $h = 10$. The x-axis denotes the m=1,...,120 minute intraday sampling (trading) frequencies.

33

Fig 9: The total potential losses, the number of observations $(T\tau)$, the expected shortfall $(ES^{(m)}_{(1-p)})$, and the Value-at-Risk $(VaR^{(m)}_{(1-p)})$, under the random walk data generated process, per sampling frequency $m = 1, ..., 120$.


Note: The left panel shows the $(\mathbb{E}(L^{(m)}))$ and the effect of size (i.e. number of observations, $T\tau$), per trading frequency $m = 1, ..., 120$, whereas the right panel shows the ES and the VaR, per trading frequency $m = 1, ..., 120$. The x-axis denotes the $m=1,...,120$ minute intraday sampling (trading) frequencies.

Fig 10: The total potential losses and kurtosis from the Student t random walk data generated process under various degrees of freedom.
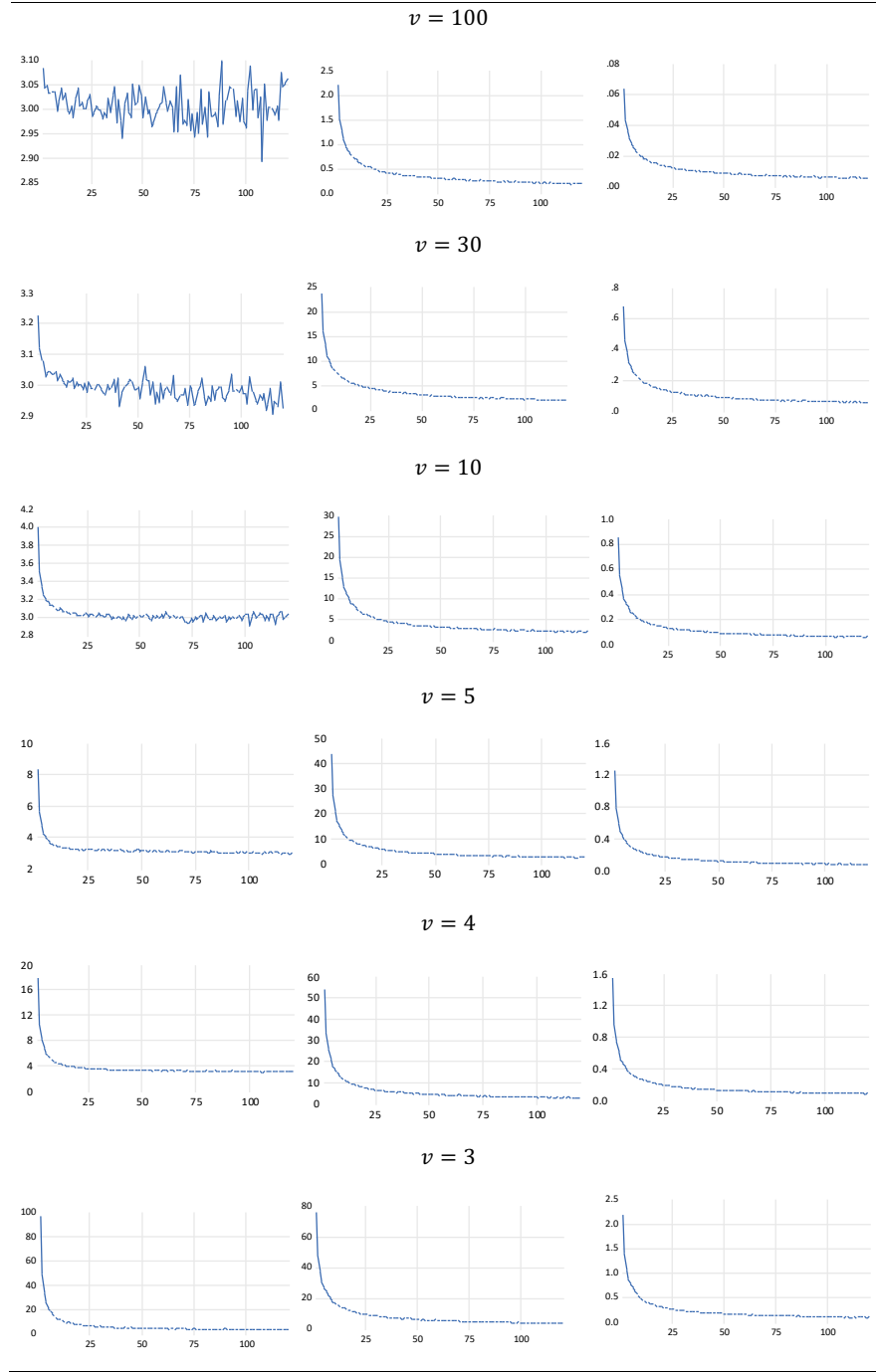
Note: The kurtosis of y_t (left panel), the potential losses $L^{(m)}$ (middle panel) and the $\bar{L}^{(m)}$ (right panel) from the Student t random walk data generated process under various degrees of freedom, v, $\log(P_t) = \log(P_{t-1}) + z_t$, $z_t \overset{i.i.d.}{\sim} t(0, 1/h^2, v)$, $P_1 = \$1,000$, $h = 10$. The x-axis denotes the $m=1,...,120$ minute intraday (trading) sampling frequencies.

Fig 11: The effect of superkurtosis on potential losses across different sampling frequencies.
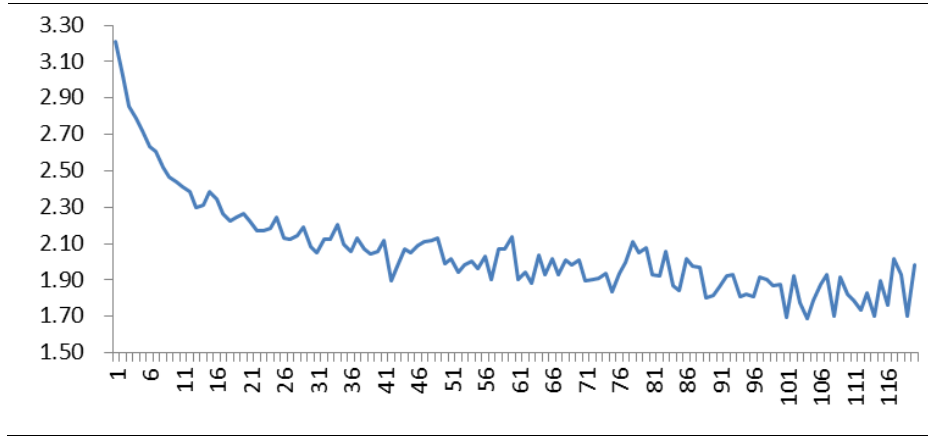
Note: The figure presents the ratio of the potential losses $(L^{(m)})$ from the Student t random walk data generated process under 3 and 30 degrees of freedom. The x-axis denotes the $m=1,...,120$ minute intraday (trading) sampling frequencies.

Appendix A: Complements to Section 2

We report some results which are referred to in the main paper, and the proof of Theorem A.2.

A.1. Construction of μ_k

In the construction of μ_k, we begin by noting that we apply the tests to demeaned data.

The first statistic to be employed is μ_2, which has been designed to test for $H_0 : E\,|X|^2 = \infty$ - i.e., the non-existence of the variance. When $k = 2$, the sample second moment (at the numerator) is made scale-invariant by dividing by the square of the mean absolute value of x_t; other rescalings would be possible (chiefly, the median, which has the advantage of being well-defined), but the simulations in Trapani (2016) show that the mean absolute value yields better power and size.

For $k = 3, 4$, rescaling is done using the sample variance, as is more natural. The rationale for these choices is also discussed in Trapani (2016). Here, we point out that we need a scale invariant test statistic - i.e. a sample moment which is not sensitive to the unit of measurement of the data. The sample variance is an obvious candidate for this, as a "natural" measure of scale. The simulations in Trapani (2016) also show that it works well in finite samples. In general, other rescalings could be considered, based on a sample moment of order lower than k. As mentioned also in Section 2, letting $p < k$, one could compute

$$\mu_p = \frac{1}{T} \sum_{t=1}^{T} |x_t|^p, \tag{A.1}$$

and then define the statistic

$$\widetilde{\mu}_k = \frac{T^{-1} \sum_{t=1}^{T} |x_t|^k}{\mu_p^{k/p}}. \tag{A.2}$$

Trapani (2016) shows that Theorem A.1 below holds for all $p < k$ (see in particular Section 3.1 in that paper).

Finally, we note that, in the formula which defines μ_k, some constants are used, denoted as c_k. These are taken directly from Trapani (2016), where they are defined as

$$c_k = \begin{cases} \frac{4}{\pi} & \text{when } k = 2 \\ 1 & \text{when } k = 3 \cdot \\ \frac{1}{3} & \text{when } k = 4 \end{cases} \tag{A.3}$$

The rationale underpinning the choice of c_k is as follows. The test works by evaluating whether a sample moment is "very large" (so that the corresponding population moment is infinite) or "sufficiently small" (which, conversely, implies that the population moment is finite). As mentioned above, the notions of being large or small are only relative notions, i.e. relative to a benchmark: Trapani (2016) argues that, letting $Z \sim N(0,1)$, a useful term of comparison for the sample k-th order moment of the data could be $c_k = E|Z|^k$.

A.2. Asymptotic behaviour of $\Theta_{T,R}^{(k)}$

Let "$\overset{d^*}{\to}$" and "$\overset{P^*}{\to}$" denote convergence in distribution and in probability, respectively, with respect to the probability conditional on the sample $\{x_t\}_{t=1}^T$, say P^*. We summarise the properties of the test above in the following theorem.[11]

Theorem A.1. *We assume that the assumptions of Theorem 1 in Trapani (2016) are satisfied, and that $R = O(T)$. Then, as $\min(T, R) \to \infty$, it holds that*

$$\Theta_{T,R}^{(k)} \overset{d^*}{\to} \chi_1^2, \ under \ H_0, \tag{A.4}$$

$$R^{-1}\Theta_{T,R}^{(k)} \overset{P^*}{\to} 1, \ under \ H_A, \tag{A.5}$$

for almost all realisations of $\{x_t\}_{t=1}^T$.

We now present a result on the behaviour of $Q^{(k)}(\alpha)$.

---

[11]The proof can be derived using exactly the same arguments as in Horváth and Trapani (2019), and we do not report it here to save space.

Theorem A.2. *We assume that the assumptions of Theorem A.1 are satisfied, and that $S = c_0 R$ for some $0 < c_0 < \infty$. Then, as $\min(T, R) \to \infty$, it holds that there exist a triple of random variables T_0, R_0, S_0 such that, for $T \geq T_0$, $R \geq R_0$ and $S \geq S_0$*

$$Q^{(k)}(\alpha) \geq (1 - \alpha) - \sqrt{\alpha(1 - \alpha)}\sqrt{\frac{2 \log \log S}{S}}, \tag{A.6}$$

under H_0, and

$$Q^{(k)}(\alpha) \leq \epsilon, \tag{A.7}$$

under H_A, for almost all realisations of $\{x_t, 1 \leq t \leq T\}$ and all $\epsilon > 0$.

Proof. We begin by noting that $E^* I\left[\Theta_{T,R,s}^{(k)} \leq c_\alpha\right] = P^*\left(\Theta_{T,R,s}^{(k)} \leq c_\alpha\right)$. From the proof of Theorem 1 in Trapani (2016) (see also more explicit calculations in Horváth and Trapani, 2019), we know that

$$\Theta_{T,R,s}^{(k)} = X_{R,s} + Y_{R,s}, \tag{A.8}$$

where

$$X_{R,s} = \left(2R^{-1/2} \sum_{j=1}^{R} \left(\zeta_{j,T,s}^{(k)}(0) - \frac{1}{2}\right)\right)^2, \tag{A.9}$$

and Horváth and Trapani (2019) show that the remainder $Y_{R,s}$ is such that $E^* Y_{R,s}^2 = c_0\left(\psi_k^{-1} + R\psi_k^{-2}\right)$ - henceforth, we omit the dependence on s when possible. Let now $\epsilon_T = \left(\psi_k^{-1} + R\psi_k^{-2}\right)^{1/3}$, and note that, using elementary arguments

$$P^*\left(\Theta_{T,R,s}^{(k)} \leq c_\alpha\right) \leq P^*\left(X_R \leq c_\alpha + \epsilon_T\right) + P^*\left(|Y_R| \geq \epsilon_T\right). \tag{A.10}$$

Thus

$$P^*\left(\Theta_{T,R,s}^{(k)} \leq c_\alpha\right) - P^*\left(X_R \leq c_\alpha\right) \tag{A.11}$$

$$\leq P^*\left(X_R \leq c_\alpha + \epsilon_T\right) - P^*\left(X_R \leq c_\alpha\right) + P^*\left(|Y_R| \geq \epsilon_T\right). \tag{A.12}$$

Markov inequality immediately yields $P^*\left(|Y_R| \geq \epsilon_T\right) \leq \epsilon_T^{-2} E^* Y_R^2 = c_0\left(\psi_k^{-1} + R\psi_k^{-2}\right)^{1/3}$. Also note that

$$P^*\left(X_R \leq c_\alpha + \epsilon_T\right) - P^*\left(X_R \leq c_\alpha\right) \tag{A.13}$$

$$= P^*\left(X_R \leq c_\alpha + \epsilon_T\right) \pm P\left(Z^2 \leq c_\alpha + \epsilon_T\right) - \left[P^*\left(X_R \leq c_\alpha\right) \pm P\left(Z^2 \leq c_\alpha\right)\right], \tag{A.14}$$

39

where $Z \sim N(0,1)$. Using Taylor's expansion, it is easy to see that

$$P\left(Z^2 \leq c_\alpha + \epsilon_T\right) - P\left(Z^2 \leq c_\alpha\right) \leq c_0 \epsilon_T. \tag{A.15}$$

Also, by the Berry-Esseen theorem (see e.g. Michel, 1976) it holds that

$$\left|P^*\left(X_R \leq c_\alpha + \epsilon_T\right) - P\left(Z^2 \leq c_\alpha + \epsilon_T\right)\right| \leq c_0 \frac{R^{-1/2}}{1 + |c_\alpha + \epsilon_T|^{3+\delta}}, \tag{A.16}$$

for all $\delta \geq 0$. Finally, using again the Berry-Esseen theorem,

$$\left|P^*\left(X_R \leq c_\alpha\right) - P\left(Z^2 \leq c_\alpha\right)\right| \leq c_0 \frac{R^{-1/2}}{1 + |c_\alpha|^{3+\delta}}. \tag{A.17}$$

Putting all together, it follows that

$$\left|P^*\left(\Theta_{T,R,s}^{(k)} \leq c_\alpha\right) - P\left(Z^2 \leq c_\alpha\right)\right| \leq c_0\left(R^{-1/2} + \epsilon_T\right). \tag{A.18}$$

Hence we have

$$\sqrt{\frac{S}{2\log\log S}} \frac{Q^{(k)}(\alpha) - (1-\alpha)}{\sqrt{\alpha(1-\alpha)}} = \sqrt{\frac{S}{2\log\log S}} \frac{S^{-1}\sum_{s=1}^{S} Z_s - (1-\alpha)}{\sqrt{\alpha(1-\alpha)}} + c_0\sqrt{\frac{S}{2\log\log S}}\left(R^{-1/2} + \epsilon_T\right),$$
$$\tag{A.19}$$

where $\{Z_s, 1 \leq s \leq S\}$ is an $i.i.d.$ sequence with common distribution $Z_1 \sim N(0,1)$. By Trapani (2016), it follows that

$$\sqrt{\frac{S}{2\log\log S}}\left(R^{-1/2} + \epsilon_T\right) = o_{a.s.}(1); \tag{A.20}$$

the desired result now follows from the Law of the Iterated Logarithm. $\qquad\square$

Appendix B: Descriptive statistics

TABLE B.1

Descriptive statistics of the three currency pairs at different sampling (trading) frequencies

Frequency	Mean	Std.Dev.	Skewness	Kurtosis	Mean	Std.Dev.	Skewness	Kurtosis
	EUR/USD futures				*EUR/USD spot*			
1m	1.34×10^{-8}	1.88×10^{-4}	1.806	729.97	8.29×10^{-8}	1.80×10^{-4}	0.337	79.58
2m	2.68×10^{-8}	2.63×10^{-4}	1.396	395.10	1.66×10^{-7}	2.55×10^{-4}	0.117	71.02
5m	6.70×10^{-8}	4.07×10^{-4}	0.799	161.38	4.14×10^{-7}	3.97×10^{-4}	0.155	45.01
10m	1.34×10^{-7}	5.69×10^{-4}	0.545	85.43	8.29×10^{-7}	5.55×10^{-4}	0.071	26.34
15m	2.01×10^{-7}	6.92×10^{-4}	0.439	62.34	1.24×10^{-6}	6.78×10^{-4}	0.353	30.59
20m	2.68×10^{-7}	7.94×10^{-4}	0.469	52.64	1.66×10^{-6}	7.78×10^{-4}	-0.001	20.03
30m	4.01×10^{-7}	9.70×10^{-4}	0.304	36.85	2.49×10^{-6}	9.51×10^{-4}	0.173	20.65
60m	8.02×10^{-7}	13.28×10^{-4}	0.271	24.67	4.97×10^{-6}	13.35×10^{-4}	0.047	13.93
Daily	8.99×10^{-5}	64.48×10^{-4}	0.033	4.33	5.93×10^{-6}	63.12×10^{-4}	0.198	6.55
	GBP/USD futures				*GBP/USD spot*			
1m	-6.52×10^{-9}	1.78×10^{-4}	-0.487	269.39	-7.92×10^{-9}	1.74×10^{-4}	-0.025	46.44
2m	-1.30×10^{-8}	2.12×10^{-4}	-0.500	119.22	-1.59×10^{-8}	2.47×10^{-4}	-0.088	48.42
5m	-3.25×10^{-8}	3.16×10^{-4}	-0.422	85.45	-3.99×10^{-8}	3.86×10^{-4}	-0.096	32.66
10m	-6.49×10^{-8}	4.42×10^{-4}	-0.364	61.41	-8.17×10^{-8}	5.41×10^{-4}	-0.107	25.23
15m	-9.76×10^{-8}	5.29×10^{-4}	-0.348	36.53	-1.23×10^{-7}	6.55×10^{-4}	-0.075	21.23
20m	-1.30×10^{-7}	6.16×10^{-4}	-0.345	41.92	-1.67×10^{-7}	7.57×10^{-4}	-0.129	24.21
30m	-1.95×10^{-7}	7.44×10^{-4}	-0.317	27.83	-2.45×10^{-7}	9.18×10^{-4}	-0.056	17.84
60m	-3.93×10^{-7}	10.14×10^{-4}	-0.288	19.71	-4.94×10^{-7}	12.91×10^{-4}	-0.113	16.15
Daily	6.22×10^{-5}	56.79×10^{-4}	-0.321	5.33	-5.96×10^{-6}	60.99×10^{-4}	0.357	8.12
	CAD/USD futures				*CAD/USD spot*			
1m	1.63×10^{-8}	1.87×10^{-4}	0.116	103.30	1.74×10^{-8}	1.97×10^{-4}	0.049	40.32
2m	3.25×10^{-8}	2.57×10^{-4}	0.067	64.32	3.48×10^{-8}	2.77×10^{-4}	-0.045	40.25
5m	8.14×10^{-8}	3.96×10^{-4}	0.029	39.46	8.59×10^{-8}	4.32×10^{-4}	-0.033	24.17
10m	1.63×10^{-7}	5.51×10^{-4}	0.049	29.89	1.73×10^{-7}	6.00×10^{-4}	-0.079	19.89
15m	2.44×10^{-7}	6.64×10^{-4}	-0.035	24.33	2.59×10^{-7}	7.34×10^{-4}	-0.002	18.88
20m	3.25×10^{-7}	7.63×10^{-4}	0.067	22.01	3.45×10^{-7}	8.41×10^{-4}	-0.038	16.45
30m	4.87×10^{-7}	9.24×10^{-4}	0.021	19.25	5.18×10^{-7}	10.26×10^{-4}	0.067	15.13
60m	9.71×10^{-7}	12.31×10^{-4}	0.192	17.48	1.03×10^{-6}	14.35×10^{-4}	0.044	14.50
Daily	5.09×10^{-5}	58.10×10^{-4}	-0.142	6.01	1.50×10^{-5}	65.76×10^{-4}	0.002	6.40